

PAPER

 View Article Online
View Journal | View Issue
Cite this: *RSC Adv.*, 2015, 5, 12277

Novel 3,6-unsymmetrically disubstituted-1,2,4,5-tetrazines: S-induced one-pot synthesis, properties and theoretical study†

 Chen Li,^{‡a} Haixia Ge,^{‡a} Bing Yin,^{ab} Mengyao She,^a Ping Liu,^{*a} Xiangdong Li^a and Jianli Li^{*a}

18 unprecedented tetrazines unsymmetrically substituted at C3 and C6 by an aromatic heterocycle have been successfully prepared by the S-induced reaction of aromatic nitriles with hydrazine hydrate under thermal conditions. The spectral property investigation suggests that compounds **4d**, **4e**, **4f**, **4p**, **4q**, **4r**, and **4v** can display intense fluorescence in the visible region, and their fluorescent properties are affected by the substituents both in tetrazine and in phenyl rings. Moreover, the electrochemical behaviors of these synthesized tetrazines are demonstrated to be fully reversible. Furthermore, density functional theory (DFT) calculations for these compounds were performed to investigate their optimized structures, Fukui function and reactivity or selectivity in the inverse electron demand Diels–Alder reaction.

 Received 19th September 2014
Accepted 14th January 2015

DOI: 10.1039/c4ra10808f

www.rsc.org/advances

Introduction

Since 1,2,4,5-tetrazine was first reported by Hantzsch and Lehmann in 1900,¹ studies of 1,2,4,5-tetrazine and its 3,6-disubstituted derivatives have received considerable attention due to their definitely unique skeleton and chemical/physical properties, and special application potential in the fields of industry, agriculture and medicine.^{2,3}

The 1,2,4,5-tetrazine ring system, which consists of an electron-deficient aromatic heterocycle with four nitrogens, is known for its high colour, biological activity and electrical property. And this system can be applied to biocompatible labelling agents,⁴ sensors,⁵ on/off fluorescence switching,⁶ live cell imaging,⁷ and components in photovoltaic cells.⁸ Additionally, the 1,2,4,5-tetrazines typically have high positive enthalpies of formation and high densities, which are suitable for the development of energetic materials with desirable properties, such as explosive, propellant and pyrotechnics.^{9,10}

As the good electron acceptors, 1,2,4,5-tetrazine derivatives can be used as 4- π components in inverse-type Diels–Alder reactions,¹¹ and provide an access to many heterocycles¹² and natural products.¹³ Furthermore, 1,2,4,5-tetrazine derivatives exhibit various biological activities such as antibacterial, antiviral and antitumor properties,^{2,14,15} therefore these compounds

can serve as pesticides, herbicides and anti-inflammatory, antimalarial drugs (Fig. 1).^{16–19}

Among many reported 1,2,4,5-tetrazine derivatives,²⁰ the 3,6-symmetrically disubstituted ones are common due to their synthetic accessibility.^{1b,13,21} In contrast, the reported 3,6-unsymmetrically disubstituted-1,2,4,5-tetrazines are limited, and especially their substituents at C3 and C6 positions are usually the alkyl and some specific substituent groups (methylthio, methoxycarbonyl and methylsulfinyl).^{11a,21,22} Furthermore, 3,6-unsymmetrically disubstituted-1,2,4,5-tetrazines with the aromatic heterocyclic substituents at C3 and C6 have rarely been reported. In addition, it is known that the substituents have an important effect on biological activities and chemical/physical properties of compounds. For 3,6-unsymmetrically disubstituted-1,2,4,5-tetrazines, the aromatic heterocyclic substituents at C3 and C6 will have the more significant effect on their spectral and electrochemical properties. Therefore, such 1,2,4,5-tetrazine derivatives may be served as potential materials with special properties. Based on this aim, we have

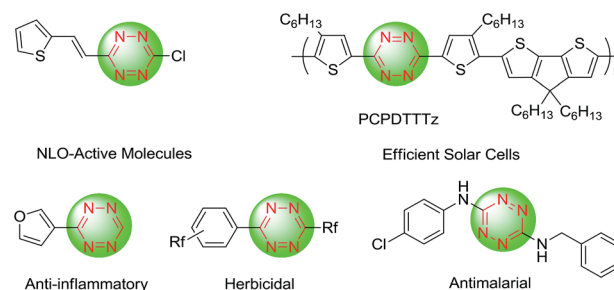


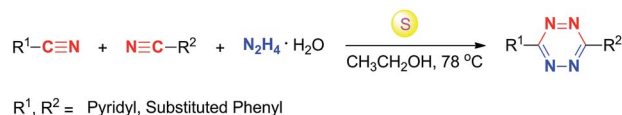
Fig. 1 The applications of tetrazines in the photonic materials and pharmacology.

^aCollege of Chemistry & Materials Science, Northwest University, Xi'an 710069, P. R. China. E-mail: lijianli@nwnu.edu.cn; liuping@nwnu.edu.cn

^bCollege of Chemistry, Beijing Normal University, Beijing 100875, P. R. China

† Electronic supplementary information (ESI) available. CCDC 973196. For ESI and crystallographic data in CIF or other electronic format see DOI: 10.1039/c4ra10808f

‡ The authors Chen Li and Haixia Ge contributed equally to this work.



Scheme 1 Preparation of 3,6-unsymmetrically disubstituted-1,2,4,5-tetrazines from nitriles and hydrazine hydrate.

devoted our recent efforts to the design and synthesis of new 3,6-unsymmetrically disubstituted-1,2,4,5-tetrazines, and the investigation of their application potential.

Herein, we detailed S-induced one-pot synthesis method for target compounds, and 18 novel 3,6-unsymmetrically disubstituted-1,2,4,5-tetrazines were first reported (Scheme 1). Moreover, the spectral and electrochemical properties²³ of obtained compounds were examined. And a systematic theoretical investigation based on the density functional theory (DFT)²⁴ calculation were carried out. Amazingly, these 1,2,4,5-tetrazines with the aromatic heterocyclic substituents at C3 and C6 positions not only can serve as special materials having both optical and electrochemical features, but also show the good reactivity or selectivity in the inverse-type Diels–Alder reaction.

Results and discussion

Synthesis

As shown in Table 1, with 2-cyano-pyridine **1a** (1.0 equivalent), 4-methylbenzonitrile **2a** (1.0 equivalent) and hydrazine hydrate **3** (10 equivalents), the optimum reaction conditions for the synthesis of the corresponding 3-(pyridin-2-yl)-6-(*p*-tolyl)-1,2,4,5-tetrazine **4a** by an intermolecular cyclization were

Table 1 Optimizing reaction conditions^a

Entry	<i>T</i> (°C)	Sulfur (equiv.)	<i>t</i> [h]	Yield ^b (%)
1	rt	0.05	9	17
2	78	0.05	9	20
3	78	0.1	9	27
4	78	1	9	34
5	78	2	9	59
6	78	4	9	72
7	78	4	5	55
8	78	4	7	63
9	78	4	10	76
10	78	4	12	80
11	78	4	14	81
12	78	0	12	0
13	58	4	12	64
14	68	4	12	73
15	88	4	12	79

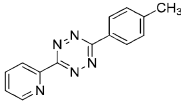
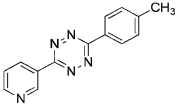
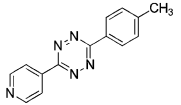
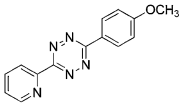
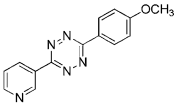
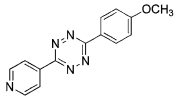
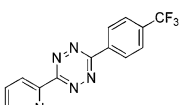
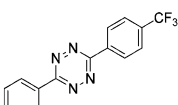
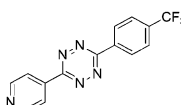
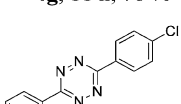
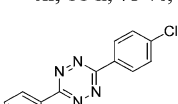
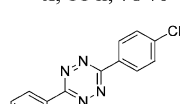
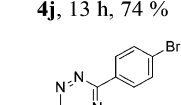
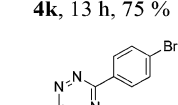
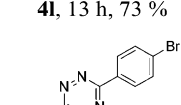
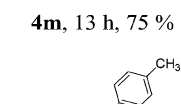
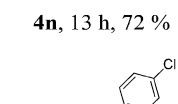
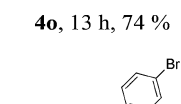
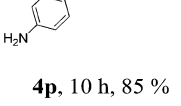
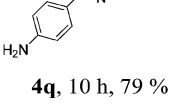
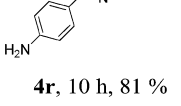
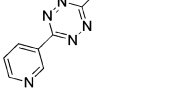
^a Reaction condition: **1a**, **2a** (each 1.0 equivalent, 0.5 mmol), hydrazine hydrate **3** (10.0 equivalents, 5.0 mmol), ethanol solution (3.0 mL), sulfur (4.0 equivalents, 2.0 mmol) at 78 °C. ^b Isolated product yields.

evaluated. We investigated the influences of reaction temperature, amount of sulfur and reaction time on the yield of product. Firstly, the CH₃CH₂OH was chosen as solvent. It is noteworthy that ethanol is not only low cost and less toxic, but also more efficient than other solvents. Then, different temperatures were examined (entries 10, 13, 14) and 78 °C was found to be the optimal temperature (entry 10). So the reaction temperature was the boiling point of ethanol, 78 °C. Moreover, the amount of sulfur was also investigated. At 78 °C, the reaction of 1.0 equivalent **1a** and **2a**, 10.0 equivalents **3** with 0.1 equivalent sulfur resulted in only 27% of product **4a** (Table 1, entry 3). When using 1.0 equivalent sulfur, the yield was improved to 34% (Table 1, entry 4). When 4.0 equivalent sulfur were used, the yield of **4a** was increased to 72% (Table 1, entry 6). These results reveal that 4.0 equivalents sulfur are suitable for this reaction. The reaction time was also tested. When the reaction time was increased to 12 h, the product **4a** was generated in 80% yield (Table 1, entry 10). Thus, the optimal condition involved the following parameters: ethanol as a solvent, reaction temperature at 78 °C, the amount of sulfur as inducer, and the reaction time.

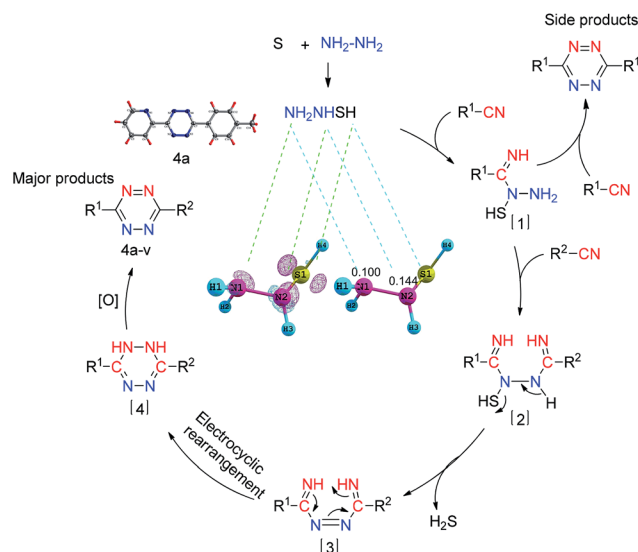
Under the optimized condition, additional aromatic nitriles were examined to expand the substrate scope, and the results are summarized in Table 2. To our delight, the reaction of various nitriles, such as cyanopyridine and substituted benzonitrile, with **3** underwent smoothly in excellent yields.

On the basis of the related literature,^{3a} a tentative mechanism for the S-induced reaction between nitriles and hydrazine hydrate, which synthesizes 3,6-unsymmetrically disubstituted-1,2,4,5-tetrazine derivatives *via* addition–elimination–rearrangement, was proposed in Scheme 2. To inducing the reaction, the S is involved in the reaction process by reacting with hydrazine hydrate to form NH₂NHSH.^{3a} The possible structure of NH₂NHSH was calculated at DFT level using double-ζ basis set (6-31G** for H element, 6-31+G* for S, N elements). Then, the NH₂NHSH interacts with nitrile to produce the key intermediate [1], and this result is supported by the Fukui function *f*_(r)[−] calculation. The *f*_(r)[−] calculation result shows that the nitrogen atom connecting with SH of the NH₂NHSH should be the first choice for the nitrile electrophilic attack since its value of condensed Fukui function (0.144) is larger than those of other atoms. The 3D representation of Fukui function *f*_(r)[−] of NH₂NHSH and the condensed *f*_(r)[−] values of N atoms of NH₂NHSH are shown in Scheme 2. The intermediate [1] further reacts with the other nitrile to generate [2]. Then, the [2] might be activated by eliminating of hydrogen sulfide to form intermediate [3]. Subsequently, the intermediate [3] converts to the [4] by electrocyclic rearrangement. Finally, the intermediate [4] converts to the target product by air oxidation. In the process of reaction, symmetrical products are also generated, but their yields are very low. The result may be arise from the fact that the concentration of R¹-CN is much lower than that of R²-CN after the intermediate [1] is produced. Then [1] more easily reacts with the nitrile with a higher concentration to form the unsymmetrical product. Thus the yield of the unsymmetrical product is much higher than that of the symmetrical product. Moreover, with a kind of nitrile as the substrate, the major product is the symmetrical tetrazines.

Table 2 Synthesis of 3,6-unsymmetrically disubstituted-1,2,4,5-tetrazines (**4a–v**) induced by **S** under thermal conditions^a

$R^1-C\equiv N + N\equiv C-R^2 + N_2H_4 \cdot H_2O \xrightarrow[CH_3CH_2OH, 78^\circ C]{S} R^1-C\equiv N-N=N-C-R^2$		
1a-d	2a-e	3
 4a , 12 h, 80 %,	 4b , 12 h, 81 %,	 4c , 12 h, 83 %,
 4d , 15 h, 80 %	 4e , 15 h, 81 %	 4f , 15 h, 79 %
 4g , 11 h, 76 %	 4h , 11 h, 75 %,	 4i , 11 h, 78 %
 4j , 13 h, 74 %	 4k , 13 h, 75 %	 4l , 13 h, 73 %
 4m , 13 h, 75 %	 4n , 13 h, 72 %	 4o , 13 h, 74 %
 4p , 10 h, 85 %	 4q , 10 h, 79 %	 4r , 10 h, 81 %
 4s , 7 h, 82 %	 4t , 7 h, 83 %	 4u , 8 h, 77 %
 4v , 7 h, 71 %		

^a Reaction condition: nitriles (each 1.0 equivalent, 0.5 mmol), hydrazine hydrate **3** (10.0 equivalents, 5.0 mmol), sulfur (4.0 equivalents, 2.0 mmol), ethanol solution (3.0 mL), at 78 °C. ^b Isolated product yields.



Scheme 2 A tentative S-induced mechanism for synthesis of 3,6-unsymmetrically disubstituted-1,2,4,5-tetrazine derivatives.

UV-vis spectroscopy

The UV-vis absorbance spectra of eight tetrazines **4d**, **4e**, **4f**, **4p**, **4q**, **4r**, **4u**, **4v** in dichloromethane lie in the ultraviolet region, and their absorption maxima are in the range of 270–346 nm (Fig. 2). Furthermore, these compounds all have an absorption maximum in the region of 317–346 nm, which belongs to the electron $n-\pi^*$ transition absorption band. For compounds **4v**, a shoulder peak can be observed around 300 nm. The maximum absorption wavelengths ($n-\pi^*$ transition) of these compounds show a certain variation regularity, which is **4d** < **4e** < **4f** < **4u**, and **4p** < **4q** < **4r** < **4v**. The result reveals that the conjugated degree increase can cause a red shift.

Fluorescence

Among all the compounds, we noticed that only **4d**, **4e**, **4f**, **4p**, **4q**, **4r**, **4u**, and **4v** can display fluorescence, and their fluorescence was shown in the visible region with the emission wavelengths lying in the range of 405–443 nm. And the fluorescence spectra and data of these compounds in dichloromethane are shown in Fig. 3 and Table 3. Moreover, the fluorescence quantum yields (Φ_f) of eight tetrazines were determined using optically matching solutions of quinine sulfate ($\Phi_f = 0.55$ in

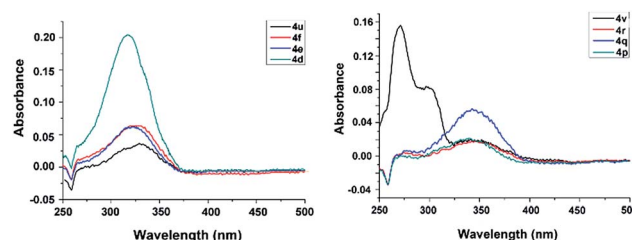


Fig. 2 UV-vis absorbance spectra of the compounds **4d**, **4e**, **4f**, **4p**, **4q**, **4r**, **4u**, and **4v** in dichloromethane ($c = 1 \times 10^{-6}$ mol L⁻¹).

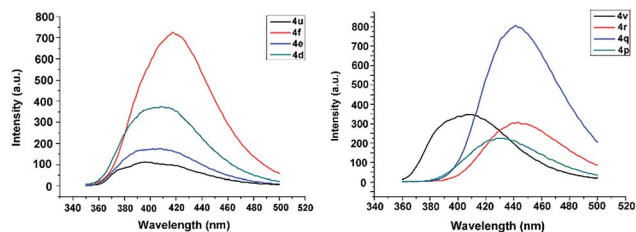


Fig. 3 Fluorescence spectra of the compounds **4d**, **4e**, **4f**, **4p**, **4q**, **4r**, **4u**, and **4v** in dichloromethane ($c = 1 \times 10^{-6}$ mol L $^{-1}$).

0.05 mol L $^{-1}$ H $_2$ SO $_4$) as standards. The quantum yields were calculated according to the related ref. 25. It is noted that these compounds with a fluorescence have the common structural character, which is the existence of an phenyl substituent (4-XC $_6$ H $_4$, X = OCH $_3$, NH $_2$) at the C3 position.

According to the phenyl substituent at C3, the eight compounds can be divided into two series: (1) **4u**, **4d**, **4e**, **4f** (–OCH $_3$ series) and (2) **4v**, **4p**, **4q**, **4r** (–NH $_2$ series). Comparison of fluorescence data of the **4u** (4-CH $_3$ OC $_6$ H $_4$) and **4v** (4-NH $_2$ C $_6$ H $_4$) show that the fluorescent wavelength of the latter is longer, since the amino group possesses stronger electron-donating ability resulting in bigger π -conjugation. Then, we compared the fluorescence data of –OCH $_3$ series **4u**, **4d**, **4e**, **4f**, and it is found that the fluorescent wavelengths of **4d**, **4e** and **4f** are longer than that of **4u**. Interestingly, this same situation exists for –NH $_2$ series compounds **4v**, **4p**, **4q** and **4r**. Furthermore, the observed change trends of fluorescent wavelengths of two series of compounds are **4f** > **4d** > **4e** > **4u** and **4r** > **4q** > **4p** > **4v**, respectively. This result could be explained by the intra-molecular charge transfer (ICT). For **4d**, **4e**, **4f** and **4p**, **4q**, **4r**, the whole molecule could form ICT from strong electron-donating groups (4-XC $_6$ H $_4$, X = OCH $_3$, NH $_2$) in C3 position to electron-withdrawing group (strong electron-withdrawing group –C $_5$ H $_5$ N (pyridyl) or weaker electron-withdrawing groups (4-XC $_6$ H $_4$, X = CH $_3$, Cl, Br)) in the C6 position, and thus the degree of π -conjugation is increased and the fluorescent wavelengths of these compounds are longer than those of **4u** and **4v**,

Table 3 Spectral data of compounds **4d**, **4e**, **4f**, **4p**, **4q**, **4r**, **4u**, and **4v** in dichloromethane

Entry	λ_{exc} , max	λ_{emi} , max ^a	Φ_u ^b
4d	335	407	0.54
4e	335	405	0.35
4f	335	418	0.67
4u	335	396	0.10
4p	344	430	0.22
4q	344	441	0.58
4r	344	443	0.37
4v	344	408	0.43

^a The fluorescence spectra of compounds **4d**, **4e**, **4f**, **4p**, **4q**, **4r**, **4u**, and **4v** in dichloromethane ($c = 1 \times 10^{-6}$ mol L $^{-1}$). The excitation slit width is 1.5 nm, the emission slit width is 3 nm. ^b Fluorescence quantum yield was determined by using quinine sulfate as a standard with $\Phi = 0.55$ in 0.05 mol L $^{-1}$ H $_2$ SO $_4$.

respectively. The above results reveal that the substituents in tetrazine and in phenyl rings both have the important effects on the fluorescence of these compounds. More importantly, the fluorescence of these compounds are in the visible range, suggesting their good application potential as the photoelectricity functional material and in photocatalyst technology.

Electrochemistry

The synthesized tetrazines unsymmetrically substituted at C3 and C6 by the aromatic heterocycle are novel and interesting compounds, which are different from those reported ones (without substituents at C3 and C6 or substituted at C3 and C6 by alkyl, specific substituent group methylthio, methoxycarbonyl, etc.) in terms of structure and properties. Especially, the synthesized tetrazines are poor solubility and remain stable in KOH environment, and this result is verified by experiment test and structure analysis. For **4a–v**, we have performed the electrochemical investigation,²⁶ which is totally different from the ones published in many closely related reports. Herein, the electrochemical test was carried out in the beaker using three-electrode system and CHI660B electrochemical workstation at room temperature. The foam nickel previously prepared was used as the working electrode. A platinum electrode and a saturated calomel electrode (SCE) were used as the counter electrode and the reference electrode, respectively. The typical CV curves for the obtained samples in 2 M KOH electrolyte *versus* SCE at scan rate of 20 mV s $^{-1}$ were well defined and fully reversible (Fig. 4).

Moreover, it is found that all the investigated tetrazines can exhibit very high reduction potentials, and the electron-rich or

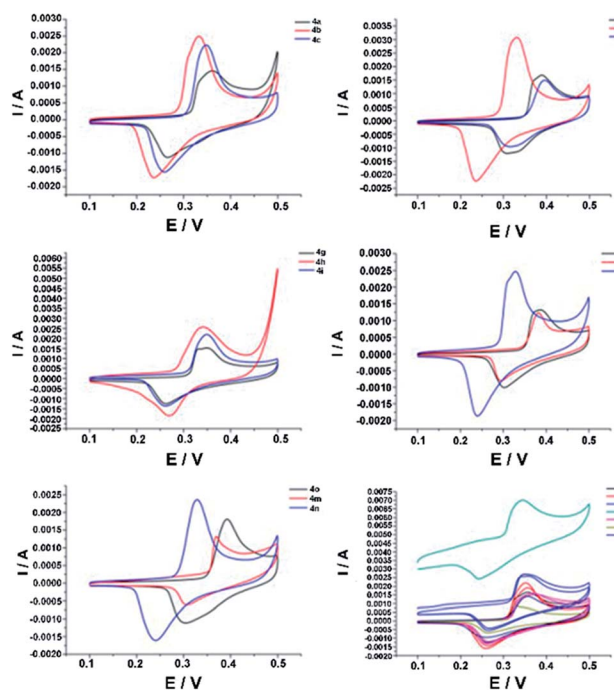


Fig. 4 Cyclic voltammetry (CV) curves for compounds **4a–v**, the obtained samples in 2 M KOH electrolyte *versus* SCE at scan rate of 20 mV s $^{-1}$, the voltage window was ranged from 0.0–0.5 V.

-poor group in the heterocyclic substituent can cause a slightly shift of the redox potential. For the reversible system, the equation as follows:

$$\Delta E_p = E_{pa} - E_{pc} = \frac{0.059}{n} \quad (1a)$$

$$E_{1/2} = (E_{pa} + E_{pc})/2 \quad (1b)$$

where E_{pa} is the oxidation potential, E_{pc} is the reduction potential, ΔE_p is the potential difference between E_{pa} and E_{pc} , $E_{1/2}$ is the half-wave potential, n is the electron transfer number. The relevant electrochemical data are listed in Table 4. As shown in Table 4, the highest reduction potential and half-wave potential were displayed by **4f**, and the lowest ones by **4e**. For **4f**, the presence of 4-pyridine and 4-methoxyphenyl made the tetrazine moiety highly electron-deficient, and this facilitated the reduction. Compounds **4a–v** exhibited high reduction potentials and half-wave potentials, which indicate that these compounds all have the high charge storage ability. The above results reveal that all compounds (**4a–v**) are potential function materials with high electrochemical energy storage ability and good electrocatalytic reduction effect.

Theoretical study

All the calculations were carried out with the Gaussian 09 program package²⁷ using the hybrid density functional theory (B3LYP) method. Basis sets of double- ζ quality (6-31G** for C, H atoms, 6-31+G* for other atoms) were used for the geometry optimization. The optimized structures were confirmed to be

local minimum due to the non-existence of imaginary frequency. Fukui function based on optimized structures has been calculated to determine the site reactivity and site selectivity.

We systematically performed calculations for all the synthesized tetrazine derivatives **4a–v**. The geometry optimization of **4a** was based on its X-ray crystal structure (Fig. 5), and the others were based on the molecular structures drawn by Chem3D and Gaussview.

To investigate the site reactivity concerning nucleophilic attack or site selectivity, the calculation of Fukui function $f_{(r)}^+$ for synthesized tetrazines was carried out.²⁸ The equation of Fukui function $f_{(r)}^+$ as follows:

$$f_{(r)}^+ = \left(\frac{\partial \rho(\vec{r})}{\partial N} \right)_v = \left(\rho(\vec{r})_{N+1} - \rho(\vec{r})_N \right)_v \quad (2a)$$

$$f_{(r)}^+ = q_x^{N+1} - q_x^N \quad (2b)$$

where N is the number of electrons, v is defined as the external potential, q_x is the electronic population of atom x in a molecule.

For **4a**, the 3D representation of the Fukui function and the condensed Fukui function of atoms are shown in Fig. 6 (**4b–v**, see in the ESI†). The 3D representation of $f_{(r)}^+$ clearly demonstrates that the region around the N atoms of the 1,2,4,5-tetrazine skeleton possess higher reactivity than other parts. Therefore the 1,2,4,5-tetrazine skeleton as the electron-deficient unit may have the stronger electrophilic ability, and can be used as the 4- π components in the inverse-type Diels–Alder reaction.

Table 4 Potential (in V vs. SCE)^a of the compounds **4a–v**

Entry	E_{pa}	E_{pc}	ΔE_p	$E_{1/2}$	n
4a	0.357	0.265	0.092	0.311	0.64
4b	0.332	0.236	0.097	0.284	0.61
4c	0.347	0.258	0.089	0.303	0.66
4d	0.389	0.309	0.080	0.349	0.74
4e	0.330	0.235	0.094	0.283	0.63
4f	0.396	0.314	0.082	0.355	0.72
4g	0.352	0.261	0.091	0.307	0.65
4h	0.340	0.270	0.070	0.305	0.84
4i	0.349	0.260	0.089	0.305	0.66
4j	0.383	0.294	0.089	0.316	0.66
4k	0.328	0.240	0.088	0.284	0.67
4l	0.384	0.302	0.082	0.343	0.72
4m	0.369	0.307	0.062	0.338	0.95
4n	0.327	0.240	0.087	0.284	0.68
4o	0.393	0.304	0.089	0.349	0.66
4p	0.370	0.260	0.110	0.315	0.54
4q	0.327	0.263	0.064	0.295	0.92
4r	0.355	0.260	0.095	0.306	0.62
4s	0.343	0.243	0.100	0.293	0.59
4t	0.350	0.265	0.085	0.308	0.69
4u	0.352	0.261	0.091	0.307	0.65
4v	0.355	0.263	0.092	0.309	0.64

^a E_{pa} represents the oxidation potential; E_{pc} represents the reduction potential; ΔE_p is the potential difference between E_{pa} and E_{pc} ; $E_{1/2}$ is the half-wave potential; n is the number of electron transferred.

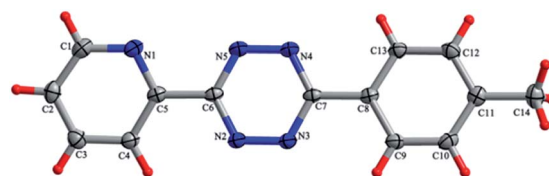


Fig. 5 X-ray crystal structure of **4a**.

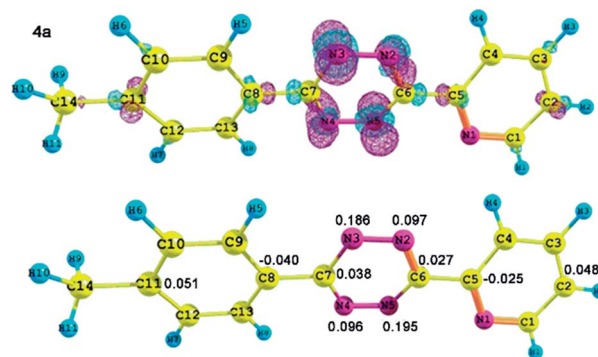


Fig. 6 3D representation of the Fukui function $f_{(r)}^+$ (positive in red color and negative in green color) and the condensed Fukui function $f_{(r)}^+$ of related atoms of **4a**.

Furthermore, the $f_{(r)}^+$ calculation results also indicate the regioselectivity in the inverse-type Diels–Alder reaction.

The frontier orbitals HOMO and LUMO for all the synthesized tetrazine derivatives have been also calculated. The 3D representations of HOMO and LUMO orbitals of **4a** are shown

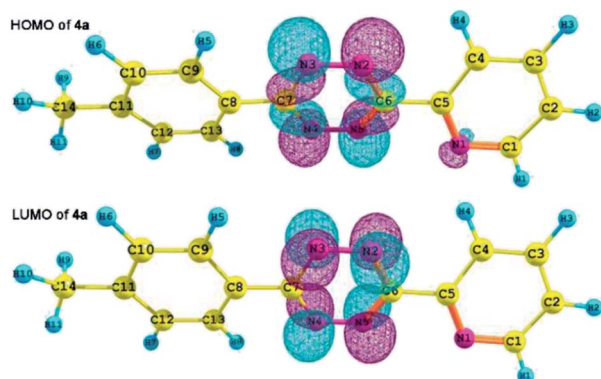


Fig. 7 3D representations of HOMO and LUMO orbitals of **4a**.

Table 5 Calculated frontier orbitals energies (eV) for **4a–v**^a

Entry	E_{HOMO}	E_{LUMO}	$\Delta E_{\text{L-H}}$
4a	−6.265	−2.746	3.52
4b	−6.455	−2.980	3.48
4c	−6.569	−3.063	3.51
4d	−6.208	−2.691	3.52
4e	−6.299	−2.926	3.37
4f	−6.406	−3.004	3.40
4g	−6.643	−3.131	3.51
4h	−6.832	−3.356	3.48
4i	−6.957	−3.445	3.51
4j	−6.491	−2.978	3.51
4k	−6.681	−3.205	3.48
4l	−6.800	−3.290	3.51
4m	−6.501	−2.988	3.51
4n	−6.691	−3.214	3.48
4o	−6.810	−3.299	3.51
4p	−5.717	−2.545	3.17
4q	−5.876	−2.752	3.12
4r	−5.882	−2.762	3.12
4s	−6.723	−3.271	3.45
4t	−6.973	−3.453	3.52
4u	−5.881	−2.618	3.26
4v	−5.435	−2.404	3.03
	−6.324	−2.832	3.49
	−8.154	−4.519	3.64
	−6.630	−3.095	3.54
	−6.337	−2.803	3.53

^a E_{HOMO} , E_{LUMO} , $\Delta E_{\text{L-H}}$ represent the energies of HOMO, LUMO, and the LUMO–HOMO gap, respectively.

in Fig. 7 (the shapes of HOMO and LUMO orbitals of **4b–v** are shown in the ESI†). The energies of HOMO, LUMO, and the LUMO–HOMO gap for **4a–v** are depicted in Table 5.

The inverse-type Diels–Alder reactions between 1,2,4,5-tetrazines and electron-rich dienes depends on the $\text{LUMO}_{\text{diene}} - \text{HOMO}_{\text{dienophile}}$ gap.²⁹ Thus for these 1,2,4,5-tetrazine derivatives as the electron-deficient dienophile, elevating their HOMO energies can facilitate the reaction. We compared the energies of HOMO, LUMO, and the LUMO–HOMO gap for **4a–v**, the result reveals that using NH_2 , CH_3O , and CH_3 as substituent can increase the HOMO energies in comparison to the CN and CF_3 , that is to say, the electron-donating substituents will increase the HOMO energies of these compounds. Moreover, we investigated the frontier molecular orbitals (FMOs) of previously reported 3,6-disubstituted-1,2,4,5-tetrazines, which have the good reactivity in the inverse-type Diels–Alder reaction.^{11d,11f,34} The HOMO energies of our tetrazine derivatives are comparable to those of the reported tetrazine derivatives, and some of them even have the higher HOMO energies than the reported ones (Table 5). Therefore, almost all of the compounds (**4a–v**) have the good potential of participating in the inverse-type Diels–Alder reaction.

Conclusions

In conclusion, tetrazines unsymmetrically substituted at C3 and C6 positions by aromatic heterocyclic groups have been systematically synthesized, and 18 novel 3,6-unsymmetrically disubstituted-1,2,4,5-tetrazines have been reported for the first time. The spectral and electrochemical properties of these synthesized tetrazines have also been investigated. These synthesized tetrazine derivatives display the intense fluorescence and fully reversible electrochemical behaviors, and the result indicate the good potential of these compounds in photonic applications. And it is found that the substituents both in tetrazine and in phenyl rings have the important effects on their spectral and electrochemical properties. In addition, the DFT calculations suggest that these synthesized tetrazines, as the electron-deficient dienophile, can exert the good reaction reactivity or selectivity in the inverse electron demand Diels–Alder reaction. The above results indicates that these 3,6-unsymmetrically disubstituted-1,2,4,5-tetrazine derivatives have the large potential to be the good lead compounds that can be used in many fields. Moreover, the further investigation of these tetrazine derivatives is warranted for developing their applications.

Experimental

General remarks

^1H NMR (400 MHz), ^{13}C NMR (100 MHz) spectra were recorded on 400 MHz spectrometers. Chemical shifts for ^1H NMR spectra are reported in parts per million downfield from TMS, chemical shifts for ^{13}C NMR spectra are reported in ppm relative to internal chloroform. Infrared spectra (IR) were recorded with KBr pellets. Silica gel (200–300 mesh) was used for column chromatography. High-resolution mass spectra were obtained

using ESI. The UV-vis absorption spectra, fluorescence spectra were recorded in dichloromethane as solvent on a UV-2520 spectrophotometer, RF-5301 PC fluorescence spectrophotometer, respectively. The single-crystal structure of **4a** was determined by X-ray crystallography (ESI†).

General procedure for the S-induced the reaction of nitriles and hydrazine hydrate

To a round-bottom flask, two kinds of nitriles (each 0.5 mmol), sulfur (64 mg, 2.0 mmol) were added to an ethanol solution (3.0 mL). Then hydrazine hydrate (250 mg, 5.0 mmol) was added in drops into the solution. The mixture was stirred overnight at the required reaction temperature. The reaction was monitored by TLC. After completion, the mixture was cooled, dichloromethane (8 mL) and water (5 mL) were added, and the sulfur was separated by the filtration. After the extraction with dichloromethane, the separated organic layer was dried over CaCl_2 , and concentrated under reduced pressure. The crude residue was purified by flash chromatography on silica gel using petroleum ether/ethyl acetate as eluent to afford the desired product.

3-(Pyridin-2-yl)-6-(*p*-tolyl)-1,2,4,5-tetrazine (**4a**)

Silica gel chromatography (petroleum ether–ethyl acetate = 2 : 1, R_f = 0.26); purple solid (99.6 mg, 80% yield); mp: 178–181 °C; ^1H NMR (400 MHz, CDCl_3) δ 8.97 (d, J = 3.4 Hz, 1H), 8.70 (d, J = 7.9 Hz, 1H), 8.60 (d, J = 8.0 Hz, 2H), 8.00 (t, J = 7.1 Hz, 1H), 7.62–7.53 (m, 1H), 7.44 (d, J = 7.9 Hz, 2H), 2.50 (s, 3H) ppm; ^{13}C NMR (100 MHz, CDCl_3) δ 164.6, 163.5, 151.1, 150.6, 144.1, 137.7, 130.4, 129.0, 128.6, 126.5, 124.0, 22.0 ppm; IR (KBr) $\nu_{\text{max}}/\text{cm}^{-1}$ 1605, 1580, 1393, 1245, 1177, 1116, 919, 812; HRMS (ESI) m/z : $[\text{M} + \text{Na}]^+$ calcd for $\text{C}_{14}\text{H}_{11}\text{N}_5 + \text{Na}^+$ 250.1093; found: 250.1093.

3-(Pyridin-3-yl)-6-(*p*-tolyl)-1,2,4,5-tetrazine (**4b**)

Silica gel chromatography (petroleum ether–ethyl acetate = 2 : 1, R_f = 0.40); purple solid (100.9 mg, 81%); mp: 197–199 °C; ^1H NMR (400 MHz, CDCl_3) δ 9.85 (s, 1H), 8.88 (dd, J = 6.6, 5.3 Hz, 2H), 8.54 (dd, J = 8.2, 5.3 Hz, 2H), 7.77 (d, J = 8.5 Hz, 1H), 7.55–7.59 (m, 1H), 7.43 (d, J = 8.0 Hz, 1H), 2.49 (s, 3H) ppm; ^{13}C NMR (100 MHz, CDCl_3) δ 164.6, 162.9, 153.3, 149.4, 144.2, 135.1, 130.4, 128.9, 128.4, 128.2, 124.2, 22.0 ppm; IR (KBr) $\nu_{\text{max}}/\text{cm}^{-1}$ 2361, 1604, 1583, 1393, 1178, 1107, 1017, 917, 849, 817, 593; HRMS (ESI) m/z : $[\text{M} + \text{Na}]^+$ calcd for $\text{C}_{14}\text{H}_{11}\text{N}_5 + \text{Na}^+$ 250.1093; found: 250.1093.

3-(Pyridin-4-yl)-6-(*p*-tolyl)-1,2,4,5-tetrazine (**4c**)

Silica gel chromatography (petroleum ether–ethyl acetate = 2 : 1, R_f = 0.39); purple solid (103.4 mg, 83%); mp: 231–233 °C; ^1H NMR (400 MHz, CDCl_3) δ 8.92 (d, J = 5.9 Hz, 2H), 8.56 (d, J = 8.2 Hz, 2H), 8.47 (d, J = 6.0 Hz, 2H), 7.43 (d, J = 8.1 Hz, 2H), 2.50 (s, 3H) ppm; ^{13}C NMR (100 MHz, CDCl_3) δ 164.6, 162.6, 151.0, 144.2, 139.2, 130.2, 128.4, 128.3, 121.0, 21.7 ppm; IR (KBr) $\nu_{\text{max}}/\text{cm}^{-1}$ 2914, 1604, 1595, 1393, 1212, 1179, 1054, 921, 828, 598; HRMS (ESI) m/z : $[\text{M} + \text{Na}]^+$ calcd for $\text{C}_{14}\text{H}_{11}\text{N}_5 + \text{Na}^+$ 250.1093; found: 250.1093.

3-(4-Methoxyphenyl)-6-(pyridin-2-yl)-1,2,4,5-tetrazine (**4d**)

Silica gel chromatography (petroleum ether–ethyl acetate = 2 : 1, R_f = 0.18); white solid (106.0 mg, 80%); mp: >270 °C; ^1H NMR (400 MHz, CDCl_3) δ 8.70 (d, J = 4.4 Hz, 1H), 8.41 (d, J = 8.0 Hz, 1H), 7.99 (d, J = 8.5 Hz, 2H), 7.88 (t, J = 7.7 Hz, 1H), 7.40 (dd, J = 12.4, 6.4 Hz, 1H), 7.02 (d, J = 8.4 Hz, 2H), 3.89 (s, 3H) ppm; ^{13}C NMR (100 MHz, CDCl_3) δ 172.2, 150.3, 150.1, 149.7, 137.4, 129.9, 125.7, 121.3, 121.2, 114.9, 100.3, 55.8 ppm; IR (KBr) $\nu_{\text{max}}/\text{cm}^{-1}$ 1606, 1517, 1437, 1408, 1307, 1249, 1173, 1115, 1029, 985, 828, 601; HRMS (ESI) m/z : $[\text{M} + \text{Na}]^+$ calcd for $\text{C}_{14}\text{H}_{11}\text{N}_5\text{O} + \text{Na}^+$ 288.0861; found: 288.0827.

3-(4-Methoxyphenyl)-6-(pyridin-3-yl)-1,2,4,5-tetrazine (**4e**)

Silica gel chromatography (petroleum ether–ethyl acetate = 2 : 1, R_f = 0.23); white solid (107.4 mg, 81%); mp: 158–159 °C; ^1H NMR (400 MHz, CDCl_3) δ 9.17 (s, 1H), 8.73 (d, J = 4.2 Hz, 1H), 8.37 (d, J = 7.9 Hz, 1H), 7.97 (d, J = 8.7 Hz, 2H), 7.46 (dd, J = 7.8, 4.9 Hz, 1H), 7.02 (d, J = 8.7 Hz, 2H), 3.89 (s, 3H) ppm; ^{13}C NMR (100 MHz, CDCl_3) δ 168.4, 163.7, 162.0, 151.4, 148.6, 134.5, 129.5, 126.5, 123.8, 122.2, 114.5, 55.3 ppm; IR (KBr) $\nu_{\text{max}}/\text{cm}^{-1}$ 1607, 1571, 1403, 1250, 1178, 1026, 835, 705.

3-(4-Methoxyphenyl)-6-(pyridin-4-yl)-1,2,4,5-tetrazine (**4f**)

Silica gel chromatography (petroleum ether–ethyl acetate = 2 : 1, R_f = 0.22); white solid (104.7 mg, 79%); mp: 164–165 °C; ^1H NMR (400 MHz, CDCl_3) δ 8.77 (d, J = 5.0 Hz, 2H), 7.97 (d, J = 8.6 Hz, 2H), 7.86 (d, J = 5.0 Hz, 2H), 7.02 (d, J = 8.6 Hz, 2H), 3.89 (s, 3H) ppm; ^{13}C NMR (100 MHz, CDCl_3) δ 169.1, 164.6, 162.1, 150.6, 137.1, 129.5, 122.1, 121.3, 114.5, 55.4 ppm; IR (KBr) $\nu_{\text{max}}/\text{cm}^{-1}$ 1598, 1400, 1313, 1179, 824, 698; HRMS (ESI) m/z : $[\text{M} + \text{H}]^+$ calcd for $\text{C}_{14}\text{H}_{11}\text{N}_5\text{O} + \text{H}^+$ 266.1042; found: 266.1049.

3-(Pyridin-2-yl)-6-(4-(trifluoromethyl)phenyl)-1,2,4,5-tetrazine (**4g**)

Silica gel chromatography (petroleum ether–ethyl acetate = 2 : 1, R_f = 0.25); purple solid (115.2 mg, 76%); ^1H NMR (400 MHz, CDCl_3) δ 9.00 (d, J = 4.2 Hz, 1H), 8.84 (d, J = 8.0 Hz, 2H), 8.73 (d, J = 7.8 Hz, 1H), 8.03 (t, J = 7.7 Hz, 1H), 7.90 (d, J = 8.0 Hz, 2H), 7.60 (t, 1H) ppm; ^{13}C NMR (100 MHz, CDCl_3) δ 163.6, 163.4, 150.9, 149.8, 137.4, 134.7, 134.5, 128.5, 126.5, 126.2, 126.1, 124.1 ppm; IR (KBr) $\nu_{\text{max}}/\text{cm}^{-1}$ 1581, 1398, 1327, 1156, 1113, 1067, 910, 825; HRMS (ESI) m/z : $[\text{M} + \text{H}]^+$ calcd for $\text{C}_{14}\text{H}_8\text{F}_3\text{N}_5 + \text{H}^+$ 304.0810; found: 304.0809.

3-(Pyridin-3-yl)-6-(4-(trifluoromethyl)phenyl)-1,2,4,5-tetrazine (**4h**)

Silica gel chromatography (petroleum ether–ethyl acetate = 2 : 1, R_f = 0.29); purple solid (113.7 mg, 75%); ^1H NMR (400 MHz, CDCl_3) δ 9.89 (s, J = 1.6 Hz, 1H), 8.93 (dq, J = 4.8, 1.6 Hz, 2H), 8.81 (d, J = 8.2 Hz, 2H), 7.91 (d, J = 8.3 Hz, 2H), 7.60 (dd, J = 7.9, 4.9 Hz, 1H) ppm; ^{13}C NMR (100 MHz, CDCl_3) δ 187.6, 163.5, 163.2, 153.5, 149.4, 135.2, 134.7, 128.4, 127.5, 126.3, 126.3, 124.0 ppm; IR (KBr) $\nu_{\text{max}}/\text{cm}^{-1}$ 1587, 1517, 1394, 1321, 1193, 1162, 1114, 1067, 909, 863, 830; HRMS (ESI) m/z : $[\text{M} + \text{H}]^+$ calcd for $\text{C}_{14}\text{H}_8\text{F}_3\text{N}_5 + \text{H}^+$ 304.0810; found: 304.0817.

3-(Pyridin-4-yl)-6-(4-(trifluoromethyl)phenyl)-1,2,4,5-tetrazine (4i)

Silica gel chromatography (petroleum ether–ethyl acetate = 2 : 1, R_f = 0.28); purple solid (118.2 mg, 78%); ^1H NMR (400 MHz, CDCl_3) δ 8.96 (d, J = 4.5 Hz, 2H), 8.83 (d, J = 8.1 Hz, 2H), 8.51 (d, J = 4.5 Hz, 2H), 7.92 (d, J = 8.2 Hz, 2H) ppm; ^{13}C NMR (100 MHz, CDCl_3) δ 163.8, 163.2, 151.2, 138.8, 134.8, 134.5, 128.6, 126.4, 126.4, 121.3 ppm; IR(KBr) $\nu_{\text{max}}/\text{cm}^{-1}$ 1633, 1400, 1325, 1170, 1132, 1067, 1108, 918, 841; HRMS (ESI) m/z : $[\text{M} + \text{H}]^+$ calcd for $\text{C}_{14}\text{H}_8\text{F}_3\text{N}_5 + \text{H}^+$ 304.0810; found: 304.0805.

3-(4-Chlorophenyl)-6-(pyridin-2-yl)-1,2,4,5-tetrazine (4j)

Silica gel chromatography (petroleum ether–ethyl acetate = 2 : 1, R_f = 0.27); purple solid (99.5 mg, 74%); mp: 218–219 °C; ^1H NMR (400 MHz, CDCl_3) δ 8.98 (d, J = 4.6 Hz, 1H), 8.70 (d, J = 7.9 Hz, 1H), 8.66 (d, J = 8.5 Hz, 2H), 8.01 (t, J = 7.7 Hz, 1H), 7.66–7.55 (m, 3H) ppm; ^{13}C NMR (100 MHz, CDCl_3) δ 164.0, 163.7, 151.2, 150.4, 139.9, 137.7, 130.2, 130.0, 129.9, 126.7, 124.2 ppm; IR(KBr) $\nu_{\text{max}}/\text{cm}^{-1}$ 2361, 1633, 1588, 1394, 1118, 1085, 913, 813; HRMS (ESI) m/z : $[\text{M} + \text{H}]^+$ calcd for $\text{C}_{13}\text{H}_8\text{ClN}_5 + \text{H}^+$ 270.0546; found: 270.0544.

3-(4-Chlorophenyl)-6-(pyridin-3-yl)-1,2,4,5-tetrazine (4k)

Silica gel chromatography (petroleum ether–ethyl acetate = 2 : 1, R_f = 0.28); purple solid (100.9 mg, 75%); mp: 217–219 °C; ^1H NMR (400 MHz, CDCl_3) δ 9.86 (s, 1H), 8.90 (t, J = 6.8 Hz, 2H), 8.63 (d, J = 8.5 Hz, 2H), 7.57–7.63 (m, 3H) ppm; ^{13}C NMR (100 MHz, CDCl_3) δ 163.9, 163.1, 153.5, 149.5, 139.9, 135.3, 130.1, 130.0, 129.6, 127.9, 124.2 ppm; IR(KBr) $\nu_{\text{max}}/\text{cm}^{-1}$ 1638, 1589, 1407, 1172, 1098, 912, 820; HRMS (ESI) m/z : $[\text{M} + \text{H}]^+$ calcd for $\text{C}_{13}\text{H}_8\text{ClN}_5 + \text{H}^+$ 270.0546; found: 270.0547.

3-(4-Chlorophenyl)-6-(pyridin-4-yl)-1,2,4,5-tetrazine (4l)

Silica gel chromatography (petroleum ether–ethyl acetate = 2 : 1, R_f = 0.28); purple solid (98.2 mg, 73%); mp: 242–243 °C; ^1H NMR (400 MHz, CDCl_3) δ 8.94 (d, J = 4.5 Hz, 2H), 8.64 (d, J = 8.0 Hz, 2H), 8.49 (d, J = 4.5 Hz, 2H), 7.63 (d, J = 8.1 Hz, 2H) ppm; ^{13}C NMR (100 MHz, CDCl_3) δ 164.49, 163.36, 151.60, 140.41, 139.41, 130.28, 130.00, 121.58, 100.38 ppm; IR(KBr) $\nu_{\text{max}}/\text{cm}^{-1}$ 1635, 1592, 1400, 1170, 1091, 1007, 915, 830; HRMS (ESI) m/z : $[\text{M} + \text{H}]^+$ calcd for $\text{C}_{13}\text{H}_8\text{ClN}_5 + \text{H}^+$ 270.0546; found: 270.0544.

3-(4-Bromophenyl)-6-(pyridin-2-yl)-1,2,4,5-tetrazine (4m)

Silica gel chromatography (petroleum ether–ethyl acetate = 2 : 1, R_f = 0.28); purple solid (117.4 mg, 75%); mp: 191–193 °C; ^1H NMR (400 MHz, CDCl_3) δ 8.98 (d, J = 4.3 Hz, 1H), 8.70 (d, J = 7.9 Hz, 1H), 8.57 (d, J = 8.3 Hz, 2H), 8.01 (t, J = 7.7 Hz, 1H), 7.77 (d, J = 8.3 Hz, 2H), 7.58 (dd, J = 7.4, 4.8 Hz, 1H) ppm; ^{13}C NMR (100 MHz, CDCl_3) δ 164.1, 163.7, 151.2, 150.3, 137.7, 132.9, 130.6, 129.9, 128.5, 126.7, 124.2 ppm; IR(KBr) $\nu_{\text{max}}/\text{cm}^{-1}$ 1584, 1393, 1116, 1066, 913, 862, 588; HRMS (ESI) m/z : $[\text{M} + \text{H}]^+$ calcd for $\text{C}_{13}\text{H}_8\text{BrN}_5 + \text{H}^+$ 314.0041; found: 314.0029.

3-(4-Bromophenyl)-6-(pyridin-3-yl)-1,2,4,5-tetrazine (4n)

Silica gel chromatography (petroleum ether–ethyl acetate = 2 : 1, R_f = 0.27); purple solid (112.7 mg, 72%); mp: 229–231 °C; ^1H NMR (400 MHz, CDCl_3) δ 9.87 (s, 1H), 8.89–8.92 (m, 2H), 8.55 (d, J = 8.6 Hz, 2H), 7.79 (d, J = 8.6 Hz, 2H), 7.58 (dd, J = 7.9, 4.9 Hz, 1H) ppm; ^{13}C NMR (100 MHz, CDCl_3) δ 164.0, 163.1, 153.4, 149.4, 135.1, 132.8, 130.4, 129.6, 128.4, 127.8, 124.1 ppm; IR(KBr) $\nu_{\text{max}}/\text{cm}^{-1}$ 1635, 1588, 1400, 1109, 914, 820, 590; HRMS (ESI) m/z : $[\text{M} + \text{H}]^+$ calcd for $\text{C}_{13}\text{H}_8\text{BrN}_5 + \text{H}^+$ 314.0041; found: 314.0036.

3-(4-Bromophenyl)-6-(pyridin-4-yl)-1,2,4,5-tetrazine (4o)

Silica gel chromatography (petroleum ether–ethyl acetate = 2 : 1, R_f = 0.28); purple solid (115.8 mg, 74%); mp: 244–247 °C; ^1H NMR (400 MHz, CDCl_3) δ 8.95 (d, J = 5.8 Hz, 2H), 8.57 (d, J = 8.6 Hz, 2H), 8.50 (d, J = 5.9 Hz, 2H), 7.80 (d, J = 8.6 Hz, 2H) ppm; ^{13}C NMR (100 MHz, CDCl_3) δ 164.3, 163.0, 151.2, 139.0, 132.9, 130.2, 129.7, 128.7, 121.2 ppm; IR(KBr) $\nu_{\text{max}}/\text{cm}^{-1}$ 1638, 1584, 1396, 1173, 1106, 1005, 920, 831, 593; HRMS (ESI) m/z : $[\text{M} + \text{H}]^+$ calcd for $\text{C}_{13}\text{H}_8\text{BrN}_5 + \text{H}^+$ 314.004; found: 314.0048.

4-(6-(*p*-Tolyl)-1,2,4,5-tetrazin-3-yl)aniline (4p)

Silica gel chromatography (petroleum ether–ethyl acetate = 3 : 1, R_f = 0.32); yellow solid (110.5 mg, 85%); mp: 180–181 °C; ^1H NMR (400 MHz, CDCl_3) δ 7.88 (d, J = 7.8 Hz, 2H), 7.81 (d, J = 8.1 Hz, 2H), 7.28 (d, J = 12.7 Hz, 2H), 6.74 (d, J = 8.1 Hz, 2H), 4.01 (s, 2H), 2.42 (s, 3H) ppm; ^{13}C NMR (100 MHz, CDCl_3) δ 168.4, 166.9, 149.4, 141.4, 130.0, 129.6, 127.9, 120.5, 115.1, 21.7 ppm; IR(KBr) $\nu_{\text{max}}/\text{cm}^{-1}$ 3130, 1600, 1516, 1401, 1261, 1098, 1019, 825.

4-(6-(4-Chlorophenyl)-1,2,4,5-tetrazin-3-yl)aniline (4q)

Silica gel chromatography (petroleum ether–ethyl acetate = 3 : 1, R_f = 0.31); yellow solid (111.8 mg, 79%); mp: 192–194 °C; ^1H NMR (400 MHz, CDCl_3) δ 7.93 (d, J = 8.5 Hz, 2H), 7.81 (d, J = 8.5 Hz, 2H), 7.46 (d, J = 8.5 Hz, 2H), 6.74 (d, J = 8.5 Hz, 2H), 4.04 (s, 2H) ppm; ^{13}C NMR (100 MHz, CDCl_3) δ 168.7, 165.2, 149.3, 136.7, 129.5, 129.3, 128.9, 128.8, 120.0, 114.8 ppm; IR(KBr) $\nu_{\text{max}}/\text{cm}^{-1}$ 3133, 1629, 1400, 1181, 1089, 821.

4-(6-(4-Bromophenyl)-1,2,4,5-tetrazin-3-yl)aniline (4r)

Silica gel chromatography (petroleum ether–ethyl acetate = 3 : 1, R_f = 0.34); yellow solid (132.4 mg, 81%); mp: 236–238 °C; ^1H NMR (400 MHz, CDCl_3) δ 7.86 (d, J = 8.2 Hz, 2H), 7.81 (d, J = 8.3 Hz, 2H), 7.62 (d, J = 8.0 Hz, 2H), 6.74 (d, J = 8.1 Hz, 2H), 4.04 (s, 2H) ppm; ^{13}C NMR (100 MHz, DMSO) δ 174.0, 169.0, 157.3, 137.5, 134.3, 134.3, 134.2, 129.3, 121.4, 118.8 ppm; IR(KBr) $\nu_{\text{max}}/\text{cm}^{-1}$ 3131, 1627, 1521, 1401, 1178, 1129, 986, 823.

3,6-Di(pyridin-3-yl)-1,2,4,5-tetrazine (4s)³⁰

Silica gel chromatography (methanol–dichloromethane = 1 : 20, R_f = 0.40); purple solid (96.8 mg, 82%); mp: 203–204 °C; ^1H NMR (400 MHz, CDCl_3) δ 9.86 (s, 2H), 8.90 (t, J = 6.6 Hz, 4H), 7.57 (dd, J = 7.8, 5.0 Hz, 2H) ppm; ^{13}C NMR (100 MHz, CDCl_3) δ

163.6, 153.7, 149.6, 135.4, 127.8, 124.3 ppm; IR(KBr) $\nu_{\text{max}}/\text{cm}^{-1}$ 1584, 1387, 1126, 1016, 917, 821, 704, 598.

3,6-Di(pyridin-4-yl)-1,2,4,5-tetrazine (4t)³¹

Silica gel chromatography (methanol–dichloromethane = 1 : 20, R_f = 0.40); purple solid (98.0 mg, 83%); mp: >200 °C; ¹H NMR (400 MHz, CDCl₃) δ 8.97 (d, J = 4.9 Hz, 4H), 8.53 (d, J = 4.9 Hz, 4H) ppm; ¹³C NMR (100 MHz, CDCl₃) δ 163.7, 151.3, 138.6, 121.4 ppm; IR(KBr) $\nu_{\text{max}}/\text{cm}^{-1}$ 2361, 1588, 1557, 1411, 1389, 1261, 1110, 1053, 921, 831, 715, 600.

3,6-Bis(4-methoxyphenyl)-1,2,4,5-tetrazine (4u)³²

Silica gel chromatography (petroleum ether–ethyl acetate = 3 : 1, R_f = 0.27); white solid (113.2 mg, 77%); mp: 170–171 °C; ¹H NMR (400 MHz, CDCl₃) δ 7.93 (d, J = 8.8 Hz, 4H), 7.00 (d, J = 8.8 Hz, 4H), 3.88 (s, 6H) ppm; ¹³C NMR (100 MHz, CDCl₃) δ 167.0, 161.7, 129.3, 122.9, 114.4, 55.4 ppm; IR(KBr) $\nu_{\text{max}}/\text{cm}^{-1}$ 2361, 1608, 1401, 1250, 1173, 987, 828.

4,4'-(1,2,4,5-Tetrazine-3,6-diyl)dianiline (4v)³³

Silica gel chromatography (petroleum ether–ethyl acetate = 1 : 1, R_f = 0.20); yellow solid (93.8 mg, 71%); mp: >280 °C; ¹H NMR (400 MHz, DMSO) δ 7.62 (d, J = 7.4 Hz, 4H), 6.66 (d, J = 7.5 Hz, 4H), 5.82 (s, 4H) ppm; ¹³C NMR (100 MHz, DMSO) δ 171.2, 156.7, 133.9, 122.1, 118.8 ppm; IR(KBr) $\nu_{\text{max}}/\text{cm}^{-1}$ 3126, 1627, 1903, 1400, 1307, 1178, 831, 776.

General procedure for preparation of solid electrode loaded test samples for electrochemical testing

The synthesized powder sample was mixed with acetylene black and caking agent polyvinylidene fluoride (PVDF) in certain proportion, and a suitable amount of anhydrous CH₃CH₂OH as demulsifier was added. And the mixture was grinded into a paste in the agate mortar, then it was besmeared on the nickel foam sheet several times (1 cm × 1.5 cm). At last, the nickel foam sheet was dried at 60 °C for 24 h and compressed with a compression stress of 10 MPa.

Acknowledgements

The project was supported by the National Natural Science Foundation of China (NSFC 21272184; 20972124; 21143010; 21103137), the Shaanxi Provincial Natural Science Fund Project (no. 2012JQ2007), the Northwest University Science Foundation for Postgraduate Students (no. YZZ13042), the Xi'an City Science and Technology Project [no. CXY1429(6); CXY1434(7)], and the Chinese National Innovation Experiment Program for University Students (no. 201210697011).

References

- (a) A. Hantzsch and M. Lehmann, *Ber. Dtsch. Chem. Ges.*, 1900, **33**, 3668; (b) J. Sauer, D. K. Heldmann, J. Hetzenegger, J. Krauthan, H. Sichert and J. Schuster, *Eur. J. Org. Chem.*, 1998, 2885.
- S. Jaiswal, P. C. Varma, L. O'Neill, B. Duffy and P. McHale, *Mater. Sci. Eng., C*, 2013, **33**, 1925.
- (a) P. Audebert, S. Sadki, F. Miomandre, G. Clavier, M. C. Vernières, M. Saoud and P. Hapiot, *New J. Chem.*, 2004, **28**, 387; (b) P. Audebert, F. Miomandre, G. Clavier, M. Vernières, S. Badré and R. Méallet-Renault, *Chem.-Eur. J.*, 2005, **11**, 5667; (c) C. Dumas-Verdes, F. Miomandre, E. Lépiciér, O. Galangau, T. Vu, G. Clavier, R. Méallet-Renault and P. Audebert, *Eur. J. Org. Chem.*, 2010, 2525; (d) N. K. Devaraj, S. Hilderbrand, R. Upadhyay, R. Mazitschek and R. Weissleder, *Angew. Chem.*, 2010, **122**, 293; (e) Z. Li, J. Ding, N. Song, X. Du, J. Zhou, J. Lu and Y. Tao, *Chem. Mater.*, 2011, **23**, 1977; (f) Q. Zhou, P. Audebert, G. Clavier, R. Méallet-Renault, F. Miomandre, Z. Shaukat, T. Vu and J. Tang, *J. Phys. Chem. C*, 2011, **115**, 21899.
- (a) N. K. Devaraj, R. Weissleder and S. A. Hilderbrand, *Bioconjugate Chem.*, 2008, **19**, 2297–2299; (b) M. L. Blackman, M. Royzen and J. M. Fox, *J. Am. Chem. Soc.*, 2008, **130**, 13518; (c) D. S. Liu, A. Tangpeerachakul, R. Selvaraj, M. T. Taylor, J. M. Fox and A. Y. Ting, *J. Am. Chem. Soc.*, 2012, **134**, 792; (d) J. Lub, W. Ten Hoeve, R. Rossin, S. M. Van Den Bosch and M. S. Robillard, WO patent, 2012049624, 2012.
- Y. Zhao, Y. Li, Z. Qin, R. Jiang, H. Liu and Y. Li, *Dalton Trans.*, 2012, **41**, 13338.
- (a) G. Clavier and P. Audebert, *Chem. Rev.*, 2010, **110**, 3299; (b) J. Malinge, C. Allain, A. Brosseau and P. Audebert, *Angew. Chem.*, 2012, **124**, 8662; (c) C. Quinton, V. Alain-Rizzo, C. Dumas-Verdes, G. Clavier, F. Miomandre and P. Audebert, *Eur. J. Org. Chem.*, 2012, 1394.
- (a) N. K. Devaraj, S. Hilderbrand, R. Upadhyay, R. Mazitschek and R. Weissleder, *Angew. Chem.*, 2010, **122**, 2931; (b) C. M. Cole, J. Yang, J. Šečutė and N. K. Devaraj, *ChemBioChem*, 2013, **14**, 205.
- Z. Li, J. Ding, N. Song, J. Lu and Y. Tao, *J. Am. Chem. Soc.*, 2010, **132**, 13160.
- (a) D. E. Chavez and M. A. Hiskey, *J. Energ. Mater.*, 1999, **17**, 357; (b) P. F. Pagoria, G. S. Lee, A. R. Mitchell and R. D. Schmidt, *Thermochim. Acta*, 2002, **384**, 187; (c) D. E. Chavez, M. A. Hiskey and R. D. Gilardi, *Org. Lett.*, 2004, **6**, 2889; (d) T. Wei, W. Zhu, X. Zhang, Y. F. Li and H. Xiao, *J. Phys. Chem. A*, 2009, **113**, 9404; (e) A. Saikia, R. Sivabalan, B. G. Polke, G. M. Gore, A. Singh, A. Subhananda Rao and A. K. Sikder, *J. Hazard. Mater.*, 2009, **170**, 306.
- (a) D. E. Chavez, M. A. Hiskey and R. D. Gilardi, *Angew. Chem.*, 2000, **112**, 1861; (b) D. E. Chavez, S. K. Hanson, J. M. Veauthier and D. A. Parrish, *Angew. Chem.*, 2013, **125**, 7014.
- (a) S. M. Sakya, K. K. Groskopf and D. L. Boger, *Tetrahedron Lett.*, 1997, **38**, 3805; (b) D. L. Boger, R. P. Schaum and R. M. Garbaccio, *J. Org. Chem.*, 1998, **63**, 6329; (c) A. Hamasaki, R. Ducray and D. L. Boger, *J. Org. Chem.*, 2006, **71**, 185; (d) H. Xie, L. Zu, H. R. Oueis, H. Li, J. Wang and W. Wang, *Org. Lett.*, 2008, **10**, 1923; (e) R. Pipkorn, W. Waldeck, B. Didinger, M. Koch, G. Mueller, M. Wiessler and K. Braun, *J. Pept. Sci.*, 2009, **15**, 235; (f) J. Schoch,

- M. Wiessler and A. Jäschke, *J. Am. Chem. Soc.*, 2010, **132**, 8846; (g) W. Chen, D. Wang, C. Dai, D. Hamelberg and B. Wang, *Chem. Commun.*, 2012, **48**, 1736.
- 12 (a) J. F. Geldard and F. Lions, *J. Org. Chem.*, 1965, **30**, 318; (b) D. L. Boger and S. M. Sakya, *J. Org. Chem.*, 1988, **53**, 1415; (c) D. L. Boger and M. Zhang, *J. Am. Chem. Soc.*, 1991, **113**, 4230; (d) R. E. Sammelson, M. M. Olmstead, M. J. Haddadin and M. J. Kurth, *J. Org. Chem.*, 2000, **65**, 9265; (e) J. C. Gonzales, T. Dedola, L. Santana, E. Uriarte, M. Begala, D. Copeze and G. Podda, *J. Heterocycl. Chem.*, 2000, **37**, 907; (f) J. Sauer, P. Bäuerlein, W. Ebenbeck, C. Gousetis, H. Sichert, T. Troll, F. Utz and U. Wallfahner, *Eur. J. Org. Chem.*, 2001, 2629; (g) J. Sauer, G. R. Pabst, U. Holland, H. Kim and S. Loebbecke, *Eur. J. Org. Chem.*, 2001, 697; (h) J. Sauer, P. Bäuerlein, W. Ebenbeck, J. Schuster, I. Sellner, H. Sichert and H. Stimmelmayer, *Eur. J. Org. Chem.*, 2002, 791; (i) L. I. Robins, R. D. Carpenter, J. C. Fettingner, M. J. Haddadin, D. S. Tinti and M. J. Kurth, *J. Org. Chem.*, 2006, **71**, 2480; (j) Y. H. Gong, P. Audebert, J. Tang, F. Miomandre, G. Clavier, S. Badré and J. Marrot, *J. Electroanal. Chem.*, 2006, **592**, 147; (k) M. J. Haddadin and E. H. Ghazvini Zadeh, *Tetrahedron Lett.*, 2010, **51**, 1654.
- 13 (a) N. Saracoglu, *Tetrahedron*, 2007, **63**, 4199; (b) D. L. Boger, C. W. Boyce, M. A. Labroli, C. A. Sehon and Q. Jin, *J. Am. Chem. Soc.*, 1999, **121**, 54; (c) D. L. Boger, D. R. Soenen, C. W. Boyce, M. P. Hedrick and Q. Jin, *J. Org. Chem.*, 2000, **65**, 2479; (d) D. L. Boger and S. E. Wolkenberg, *J. Org. Chem.*, 2000, **65**, 9120; (e) D. L. Boger and J. Hong, *J. Am. Chem. Soc.*, 2001, **123**, 8515; (f) Z. Wan, G. H. C. Woo and J. K. Snyder, *Tetrahedron*, 2001, **57**, 5497.
- 14 A. Borkowski, M. Szala and D. Wolicka, *Chem. Ecol.*, 2011, **27**, 57.
- 15 W. Hu, G. Rao and Y. Sun, *Bioorg. Med. Chem. Lett.*, 2004, **14**, 1177.
- 16 (a) J. Hajimichael, S. Botar, E. Bleicher, L. Pap, I. Szekely and K. Marmarosi, US pat., 5455237, 1995; (b) J. Hajimichael, D. Botár, E. Bleicher, D. Pap, D. Székely, N. K. K. Mármárosi and J. Ori, EP patent, 0635499, 1999.
- 17 K. H. Pilgram, L. E. Wittsell, R. D. Skiles, A. L. James and J. W. Dawson, *J. Agric. Food Chem.*, 1977, **25**, 888.
- 18 S. A. Lang Jr, B. D. Johnson, E. Cohen, A. E. Sloboda and E. Greenblatt, *J. Med. Chem.*, 1976, **19**, 1404.
- 19 D. Nhu, S. Duffy, V. M. Avery, A. Hughes and J. B. Baell, *Bioorg. Med. Chem. Lett.*, 2010, **20**, 4496.
- 20 (a) J. Yang, M. R. Karver, W. Li, S. Sahu and N. K. Devaraj, *Angew. Chem., Int. Ed.*, 2012, **51**, 5222; (b) W. W. Zajac Jr, J. F. Siuda, S. M. J. Nolan and T. M. Santosusso, *J. Org. Chem.*, 1971, **36**, 3539; (c) N. O. Abdel, M. A. Kira and M. N. Tolba, *Tetrahedron Lett.*, 1968, **9**, 3871; (d) C. L. Lim, S. H. Pyo, T. Y. Kim, E. S. Yim and B. H. Han, *Bull. Korean Chem. Soc.*, 1995, **16**, 374; (e) M. D. Coburn, G. A. Buntain, B. W. Harris, M. A. Hiskey, K. Y. Lee and D. G. Ott, *J. Heterocycl. Chem.*, 1991, **28**, 2049.
- 21 K. Pilgram and R. D. Skiles, *J. Org. Chem.*, 1976, **41**, 3392.
- 22 W. Hu and F. Xu, *J. Heterocycl. Chem.*, 2008, **45**, 1745.
- 23 P. Audebert, F. Miomandre, G. Clavier, M. C. Vernières, S. Badré and R. Méallet-Renault, *Chem.-Eur. J.*, 2005, **11**, 5667.
- 24 (a) Z. Bayat, S. Daneshnia and S. J. Mahdizadeh, *Phys. E*, 2011, **43**, 1569; (b) M. Moral, G. García, A. Peñas, A. Garzón, J. M. Granadino-Roldán, M. Melguizo and M. Fernández-Gómez, *Chem. Phys.*, 2012, **408**, 17; (c) M. Plugge, V. Alain-Rizzo, P. Audebert and A. M. Brouwer, *J. Photochem. Photobiol., A*, 2012, **234**, 12.
- 25 (a) X. Li, G. Zhang, H. Ma, D. Zhang, J. Li and D. Zhu, *J. Am. Chem. Soc.*, 2004, **126**, 11543; (b) J. R. Lakowicz, in *Principles of Fluorescence Spectroscopy*, Kluwer Academic/Plenum, New York, 2nd edn, 1999.
- 26 M. L. Li, W. W. Xu, W. R. Wang, Y. P. Liu, B. Cui and X. H. Guo, *J. Power Sources*, 2014, **248**, 465.
- 27 M. J. Frisch, G. W. Trucks, H. B. Schlegel, G. E. Scuseria, M. A. Robb, J. R. Cheeseman, G. Scalmani, V. Barone, B. Mennucci, G. A. Petersson, H. Nakatsuji, M. Caricato, X. Li, H. P. Hratchian, A. F. Izmaylov, J. Bloino, G. Zheng, J. L. Sonnenberg, M. Hada, M. Ehara, K. Toyota, R. Fukuda, J. Hasegawa, M. Ishida, T. Nakajima, Y. Honda, O. Kitao, H. Nakai, T. Vreven, J. A. Montgomery Jr, J. E. Peralta, F. Ogliaro, M. Bearpark, J. J. Heyd, E. Brothers, K. N. Kudin, V. N. Staroverov, R. Kobayashi, J. Normand, K. Raghavachari, A. Rendell, J. C. Burant, S. Iyengar, J. Tomasi, M. Cossi, N. Rega, J. M. Millam, M. Klene, J. E. Knox, J. B. Cross, V. Bakken, C. Adamo, J. Jaramillo, R. Gomperts, R. E. Stratmann, O. Yazyev, A. J. Austin, R. Cammi, C. Pomelli, J. W. Ochterski, R. L. Martin, K. Morokuma, V. G. Zakrzewski, G. A. Voth, P. Salvador, J. J. Dannenberg, S. Dapprich, A. D. Daniels, O. Farkas, J. B. Foresman, J. V. Ortiz, J. Cioslowski and D. J. Fox, in *Gaussian 09, Revision A.02*, Gaussian, Inc., Wallingford CT, 2009.
- 28 (b) D. Qi, L. Zhang, L. Wan, Y. Zhang, Y. Bian and J. Jiang, *Phys. Chem. Chem. Phys.*, 2011, **13**, 13277; (c) D. Qi, L. Zhang, L. Zhao, X. Cai and J. Jiang, *ChemPhysChem*, 2012, **13**, 2046.
- 29 J. Balcar, G. Chrisam, F. X. Huber and J. Sauer, *Tetrahedron Lett.*, 1983, **24**, 1481.
- 30 J. Spanget-Larsen, E. W. Thulstrup and J. Waluk, *Chem. Phys.*, 2000, **254**, 135.
- 31 J. Li, Y. Peng, H. W. Liang, Y. Yu, B. J. Xin, G. H. Li, Z. Shi and S. H. Feng, *Eur. J. Inorg. Chem.*, 2011, 2712.
- 32 M. Plugge, V. Alain-Rizzob, P. Audebert and A. M. Brouwer, *J. Photochem. Photobiol., A*, 2012, **234**, 12.
- 33 A. R. Katritzky, J. Soloducho and S. Belyakov, *ARKIVOC*, 2000, **1**, 37.
- 34 R. A. Caboni and R. V. Lindsey, Jr, *J. Am. Chem. Soc.*, 1959, **81**, 4342.